Developmental Biology 449 (2019) 41–51

Contents lists available at ScienceDirect

Developmental Biology

journal homepage: www.elsevier.com/locate/developmentalbiology

Transcriptional and post-transcriptional regulation of *extra macrochaetae* during *Drosophila* adult peripheral neurogenesis

Ke Li [a,1], Nicholas E. Baker [a,b,c,*]

[a] Department of Genetics, Albert Einstein College of Medicine, 1300 Morris Park Avenue, Bronx NY 10461, USA
[b] Department of Developmental and Molecular Biology, Albert Einstein College of Medicine, 1300 Morris Park Avenue, Bronx NY 10461, USA
[c] Department of Ophthalmology and Visual Sciences, Albert Einstein College of Medicine, 1300 Morris Park Avenue, Bronx NY 10461, USA

A B S T R A C T

Regulation of the *Drosophila* ID protein Extra macrochaetae (Emc) is important because reduced Emc levels have been proposed to favor proneural gene activity and thereby define a prepattern for neurogenesis. Recent studies suggest a major role for post-translational control of Emc levels. To further define the mechanisms of Emc regulation, we identified two redundant *cis*-regulatory regions by germline transformation-rescue experiments that make use of new molecularly-defined *emc* mutants. We distinguished the mechanisms by which Daughterless (Da) regulated Emc expression, finding post-translational regulation in most tissues, and additional transcriptional regulation in the eye imaginal disc posterior to the morphogenetic furrow. Dpp and Hh signaling pathways repressed Emc transcriptionally and post-translationally within the morphogenetic furrow of the eye disc, whereas Wg signaling repressed Emc expression at the anterior margin of the wing imaginal disc. Although the *emc* 3′ UTR is potentially regulatory, no effect of miRNA pathways on Emc protein levels was discernible. Our work supports recent evidence that post-transcriptional mechanisms contribute more to regulation of Emc protein levels than transcriptional mechanisms do.

1. Introduction

The *extra macrochaetae* (*emc*) gene was discovered as a negative regulator of proneural basic-helix-loop-helix (bHLH) proteins of the Achaete-Scute Complex (AS-C) (Botas et al., 1982), and found to encode the *Drosophila* homolog of the Inhibitor of DNA binding (ID) gene family (Garrell and Modolell, 1990). Emc/ID proteins act as dominant negative antagonists of bHLH transcription factors by forming heterodimers that are unable to bind DNA, and therefore are involved in a multitude of development events including neurogenesis, myogenesis and hematopoiesis (Benezra et al., 1990; Ellis, 1994; Massari and Murre, 2000; Murre, 2019). The pattern of *emc* expression has been proposed to define a negative prepattern for neurogenesis, such that proneural gene function is enhanced and neural determination favored where *emc* expression is low (Cubas and Modolell, 1992; Bhattacharya and Baker, 2011; Troost et al., 2015). The neural prepattern is thought to make a significant contribution to neural patterning. The proneural bHLH proteins of the AS-C, although both necessary and sufficient for much neural fate specification in *Drosophila,* are surprisingly ineffective at reprogramming imaginal disc cells to neural fate when misexpressed, presumably because their full activity is determined by the distribution of other factors such as Emc (Rodriguez et al., 1990; Bhattacharya and Baker, 2011). This may be relevant to efforts to reprogram human cells into neurons therapeutically, which may be limited by the effectiveness of ectopic proneural gene expression (Guillemot and Hassan, 2017; Jorstad et al., 2017).

Although expressed widely in *Drosophila* tissues, Emc levels are reduced in the morphogenetic furrow of the developing eye imaginal discs, and along the primordium of the anterior wing margin in the wing imaginal discs, two proneural regions where sensory neurons are specified (Brown et al., 1995; Bhattacharya and Baker, 2011). The *emc* mRNA also accumulates to different levels in a complex pattern. In *Drosophila* wing imaginal discs, eye imaginal discs, and follicular epithelia, *emc* transcription is elevated by Notch signaling, and is proposed to contribute to Notch function in those tissues (Cubas and Modolell, 1992; Baonza et al., 2000; Adam and Montell, 2004; Bhattacharya and Baker, 2009). Another regulator of *emc* transcription is the bHLH protein Daughterless (Da), the ubiquitously-expressed heterodimer partner of proneural bHLH proteins. Over-expression of Da stimulates *emc* transcription, whereas *da* gene function is required to maintain Emc expression in most or all tissues, at least at the level of Emc protein (Bhattacharya and Baker, 2011). Because *emc* is itself a repressor of Da expression, at least at the Da protein level, Emc protein has the potential to act as a negative feedback regulator of Da activity (Bhattacharya and

* Corresponding author. Department of Genetics, Albert Einstein College of Medicine, 1300 Morris Park Avenue, Bronx NY 10461, USA.
E-mail address: nicholas.baker@einstein.yu.edu (N.E. Baker).
[1] Present address: Howard Hughes Medical Institute, Department of Physiology, University of California, San Francisco, San Francisco, CA 94158.

https://doi.org/10.1016/j.ydbio.2019.02.003
Received 18 July 2018; Received in revised form 11 February 2019; Accepted 11 February 2019
Available online 13 February 2019

Baker, 2011). Negative feedback relationships have also been documented between mammalian ID proteins and mammalian E-protein genes, the homologs of *Drosophila* Da (Bhattacharya and Baker, 2011; Schmitz et al., 2012).

Given extensive evidence of regulated *emc* transcription, it was surprising to find that the *emc* null phenotype can be rescued substantially by uniform transcription of UAS-*emc* transgenes using the actin-Gal4 driver (Li and Baker, 2018). This may be made possible by regulation of Emc expression at the post-transcriptional level. In particular, Emc protein is unstable when not heterodimerized with Da, and proneural bHLH proteins may modify Emc stability by competing with the stable Emc-Da heterodimer that is apparently present in most cells (Li and Baker, 2018). These recent findings regarding post-translational regulation raise the question of the significance of *emc* mRNA levels and their regulation.

To help address the contributions of various levels of regulation to *emc* function, here we have explored the regulation of *emc* mRNA levels. Previously, the extent of the *emc* gene regulatory region had not been mapped. Except for the predicted gene *hinge3* (*hng3*) transcribed on the opposite strand, *emc* is separated from the nearest other Pol-II transcription units by 37 kb on the 5' (centromere distal) side and 48 kb on the 3' (centromere proximal) side. Such large gaps between genes suggest the presence of extended regulatory sequences. Accordingly, chromosome rearrangements with breakpoints far from the *emc* transcription unit are *emc* mutant alleles (Garrell and Modolell, 1990). Potential regulatory sequences close to the *emc* transcription unit direct only limited patterns of expression, much more restricted than the *emc* mRNA itself (Spratford and Kumar, 2015). On the other hand, most P-element insertions causing *emc* mutations were recovered in the close proximity to the *emc* transcription unit (Ellis et al., 1990; Garrell and Modolell, 1990). The *emc* transcript contains a long 3′ UTR, and is predicted to be a target of many microRNAs (miRNAs), although the effect of miRNAs on Emc expression has not been tested. Interestingly, the gain-of-function emc^{D} allele contains a transposable element insertion into the last exon that presumably results in *emc* transcripts lacking the normal 3′-UTR, and shows elevated levels of *emc* mRNA (Garrell and Modolell, 1990; Cubas and Modolell, 1992).

Here we provide evidence for multiple transcriptional regulatory regions flanking both sides of the *emc* gene, and also evidence that other important sequences map further away from the transcription unit. We successfully generated two new molecularly-defined protein null alleles of *emc*. We confirmed that *da* is required for *emc* transcription, but only in particular regions, whereas Emc post-transcriptional regulation is more general. In the morphogenetic furrow of the eye disc, Hh and Dpp repress *emc* transcription in addition to regulating Emc protein stability. At the anterior wing margin, Wg represses Emc expression, possibly through Senseless (Sens). We also present evidence that the miRNA machinery may not contribute significantly to Emc protein levels. Altogether, our results suggested that although *emc* receives transcriptional inputs from different pathways in a context-dependent manner, Emc expression is primarily regulated post-transcriptionally, probably at the level of protein stability.

2. Results

2.1. Significant regulatory information lies in the vicinity of the emc transcription unit

Two ~20 kb genomic BAC clones CH322-19P18 and CH322-98H21 (named 19P18 and 98H21 for short, respectively) (Venken et al., 2009), each of which contains the whole *emc* transcription unit and ~15 kb upstream or downstream sequences, were used to make transgenic flies and assessed for rescue of an *emc* null genotype, emc^{AP6}/Df (Fig. 1A and B). emc^{AP6} is a protein-null allele induced by P-M hybrid dysgenesis and associated with a deletion of approximately 400bp of coding sequences (Ellis, 1994). BAC 19P18 has–10 kb of unique upstream sequence and 98H21 has–13 kb of unique downstream sequence, in addition to ~8 kb encompassing the *emc* transcription unit that is present in both BACs (Fig. 1A and B).

We found that genomic transgenes for either of 19P18 and 98H21 rescued the embryonic lethality of *emc* nulls and all the rescued flies showed grossly normal morphology as pharate adults (Fig. S1C–D and S1F-G). However, rescued flies failed to eclose from pupal cases, and the pharate adults had extra thoracic bristles, resembling an *emc* hypomorphic phenotype (Fig. S1D and S1G). We then tested whether these two genomic regions together could rescue the *emc* mutants, as would be expected if they each supplied complementary aspects of *emc* expression. Although double transgenic flies were rescued as well as each single transgenic, reaching pharate adulthood with largely normal morphology, they still had extra thoracic bristles and adults failed to emerge (Fig. 1C, E, G and I). These data suggested that each of the 19P18 and 98H21 genomic segments contained significant *emc* regulatory information, although apparently not complete.

Because Emc is involved in regulating Da expression and neurogenesis, we next examined the proneural regions in the rescued eye and wing imaginal discs where Da and Emc are regulated dynamically but remained relatively homogenous otherwise (Fig. 1D and H and Fig. S1A). Consistently, all the rescued eye and wing discs exhibited fairly normal Emc expression patterns including lower Emc level in the proneural regions of the morphogenetic furrow and the anterior wing margin (Fig. 1F, Fig. S1B, E and H). Sometimes the level of Da in the proneural regions was less evidently raised than in wild type (Fig. S1H). We also found that rescued flies performed neurogenesis normally in the eye imaginal discs, as indicated by normal Elav labeling in differentiating photoreceptor cells (Fig. 1F, Fig. S1E and S1H). As the rescued pharate adults had extra thoracic bristles, we also carefully examined the corresponding nota. The Emc level in the rescued nota was not reduced overall compared to that in wild type (Fig. 1H and J). However, the rescued nota generally had patches of cells with lower Emc expression. Da levels were higher in these patches, in which ectopic sensory organ precursors arose (Fig. 1J). Taken together, these results confirmed that the 35 kb region covered by the two BAC clones contained important regulatory elements of the *emc* gene, but perhaps not all.

Because the 19P18 and 98H21 genomic clones each rescued *emc* mutants to similar extents, the simple interpretation was that the 8 kb regions shared by both BACs contained the relevant regulatory elements. To test this, we generated transgenic flies carrying a 10 kb genomic transgene that covered the common regions between two BACs (Fig. 1B). This 10 kb transgene failed to rescue embryonic lethality of emc^{AP6}/Df, however, and made no additional contribution when combined with either 19P18 or 98H21 (data not shown). These findings indicated that 19P18 and 98H21 each contained distinct regulatory elements outside of their common region, either one of which was sufficient for the significant rescue seen in the transgenic flies. The lack of additional rescue in emc^{AP6}/Df flies carrying both 19P18 and 98H21 suggested that these regulatory sequences functioned redundantly.

2.2. Generation and characterization of molecularly defined emc amorphic alleles

The failure of the 19P18/98H21 transgenic combination that includes 35 kb of potential regulatory DNA to completely rescue could be explained by requirement for additional, more distant regulatory regions. Alternatively, the emc^{AP6}/Df genotype might contain linked mutations in another gene. The emc^{AP6} allele was generated by random P-M dysgenesis and may carry additional mutations. Moreover, the ~400bp deletion in emc^{AP6} affects an intron of the predicted gene *hng3* encoded on the opposite strand. Neither the 19P18 nor the 98H21 BAC clones includes a complete *hng3* transcription unit and would not be expected to rescue any defect in this gene (Fig. 1A). To distinguish these possibilities, we sought to generate additional *emc* null alleles using the CRISPR technique. Our goal was to make a small deletion shortly after the translation start site,

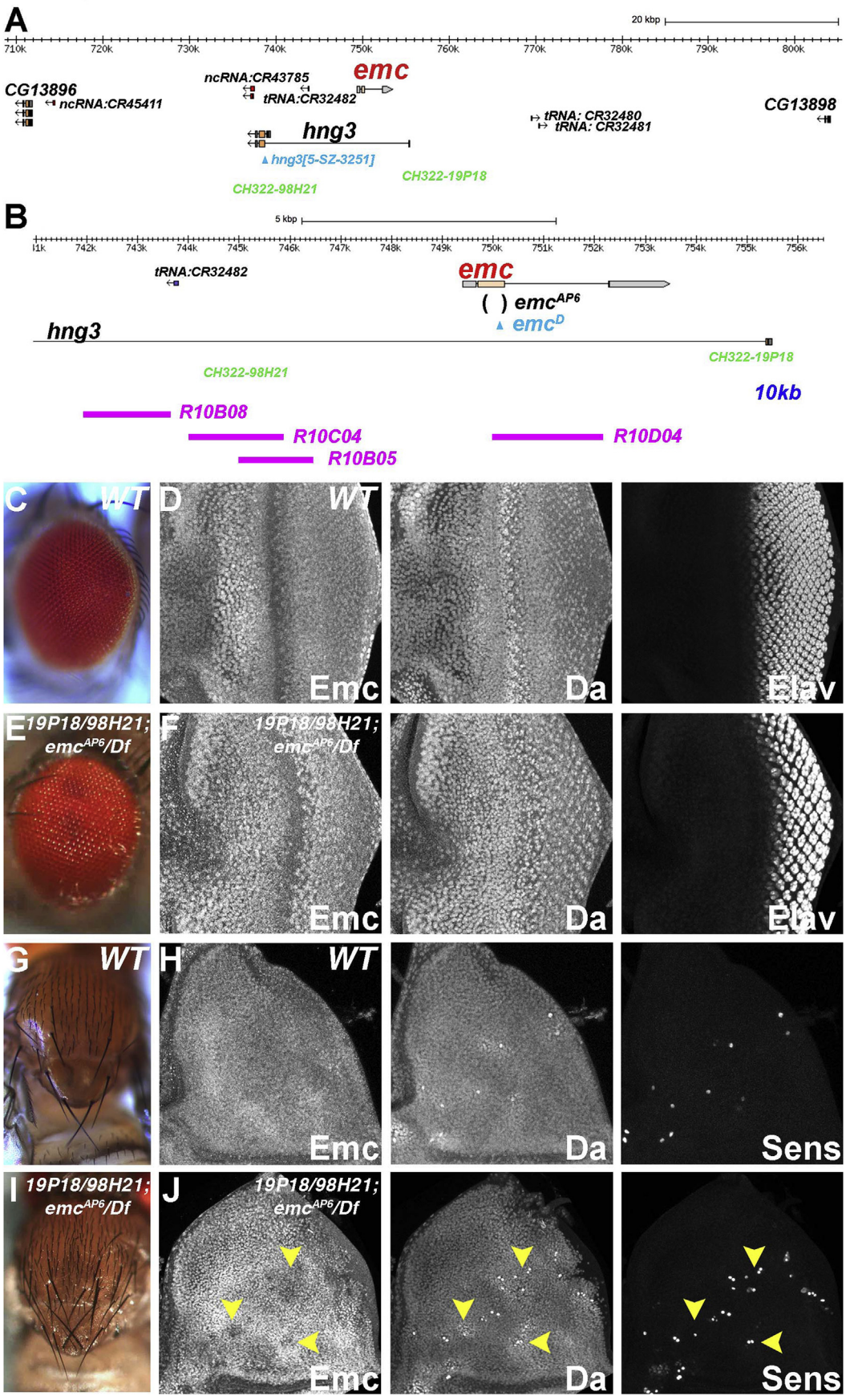

(caption on next page)

Fig. 1. Functional analysis of the *emc* locus. (A) A diagram showing the genomic regions around the *emc* transcription unit between its nearest upstream and downstream coding genes. The two genomic BAC clones used to make transgenic flies are shown in green. Note the predicted gene *hng3* on the opposite strand with the blue arrow indicating the P-element insertion near its splice acceptor site. (B) A close-up around the *emc* region that is shared by the two BAC clones. The 10 kb genomic transgene is shown in dark blue. The bracket depicts the ~400bp coding sequence deleted in the emc^{AP6} allele and the light blue arrow indicates where the transposon inserted in the emc^{D} allele. Four Janelia Farm Gal4 lines are shown in magenta, each of which contains a genomic fragment around the *emc* locus. Panels (A,B) were modified from Flybase Genome Browser pages (Thurmond et al., 2019). (C–J) Adult (C, E, G, I) and larval (D, F, H, J) tissues of wild type (C-D and G-H) and emc^{AP6}/Df transheterozygous mutant rescued by BAC clones 19P18 and 98H21 (E-F and I-J). (C) Wild type adult eye showing normal ommatidia. (D) Immunofluorescence labeling of wild type eye imaginal discs showing broad expression Da and Emc proteins. Elav labels differentiated photoreceptor neurons. (E) Rescued flies fail to eclose but arrest at a late stage of pharate adult development. The rescued pharate adult fly eyes appear morphologically normal. (F) Emc, Da and Elav expression patterns appear largely normal in eye discs from the rescued larvae (although the upregulation of Da normally seen in wild type morphogenetic furrow is sometimes less evident). (G) Wild type thorax displays 11 pairs macrochaetae (7 pairs are shown here) and evenly-spaced microchaetae. (H) Wild type larval notum showing single sensory organ precursor (SOP) cells labeled by Sens. Emc and Da proteins are expressed widely, although the SOP cells generally have lower Emc and higher Da. (I) The rescued adult flies have extra bristles (yellow arrows) on the thoraxes. (J) Emc and Da are also broadly detected in nota from the rescued larvae. Patches of cells (yellow arrowheads) with lower Emc expression are often observed, which also display higher Da expression and extra SOP cells marked by Sens. Genotype: (C-D and G-H) w^{1118}, (E-F and I-J) *PBac{19P18, w+}/PBac{98H21,w+};* $emc^{AP6}/Df(3L)ED202$.

frameshifting the *emc* open reading frame with minimal impact on *hng3* or other genes (Fig. 2A).

Two novel *emc* alleles were recovered (see Methods for details). We sequenced both alleles and found deletions of 1 bp and 5 bp, respectively (Fig. 2B), both of which frameshift the *emc* open reading frame. The two new CRISPR alleles were named $emc^{\Delta 1}$ and $emc^{\Delta 5}$, respectively. No Emc protein was detected in clones of cells homozygous for the $emc^{\Delta 1}$ or $emc^{\Delta 5}$ alleles in eye or wing imaginal discs, consistent with both corresponding to a protein null alleles of *emc* (Fig. 2C and D).

To further characterize $emc^{\Delta 1}$ and $emc^{\Delta 5}$, we examined some loss-of-function phenotypes. As reported previously for the emc^{AP6} mutation (Bhattacharya and Baker, 2011), high Da levels were observed in the $emc^{\Delta 1}$ clones (Fig. 2C and D). We used the eyFlp/Minute technique to obtain third instar eye discs that were largely mutant for $emc^{\Delta 1}$. As reported previously for emc^{AP6} (Bhattacharya and Baker, 2009) (Figs. S2A–B), the $emc^{\Delta 1}$ eye discs exhibited accelerated progression of

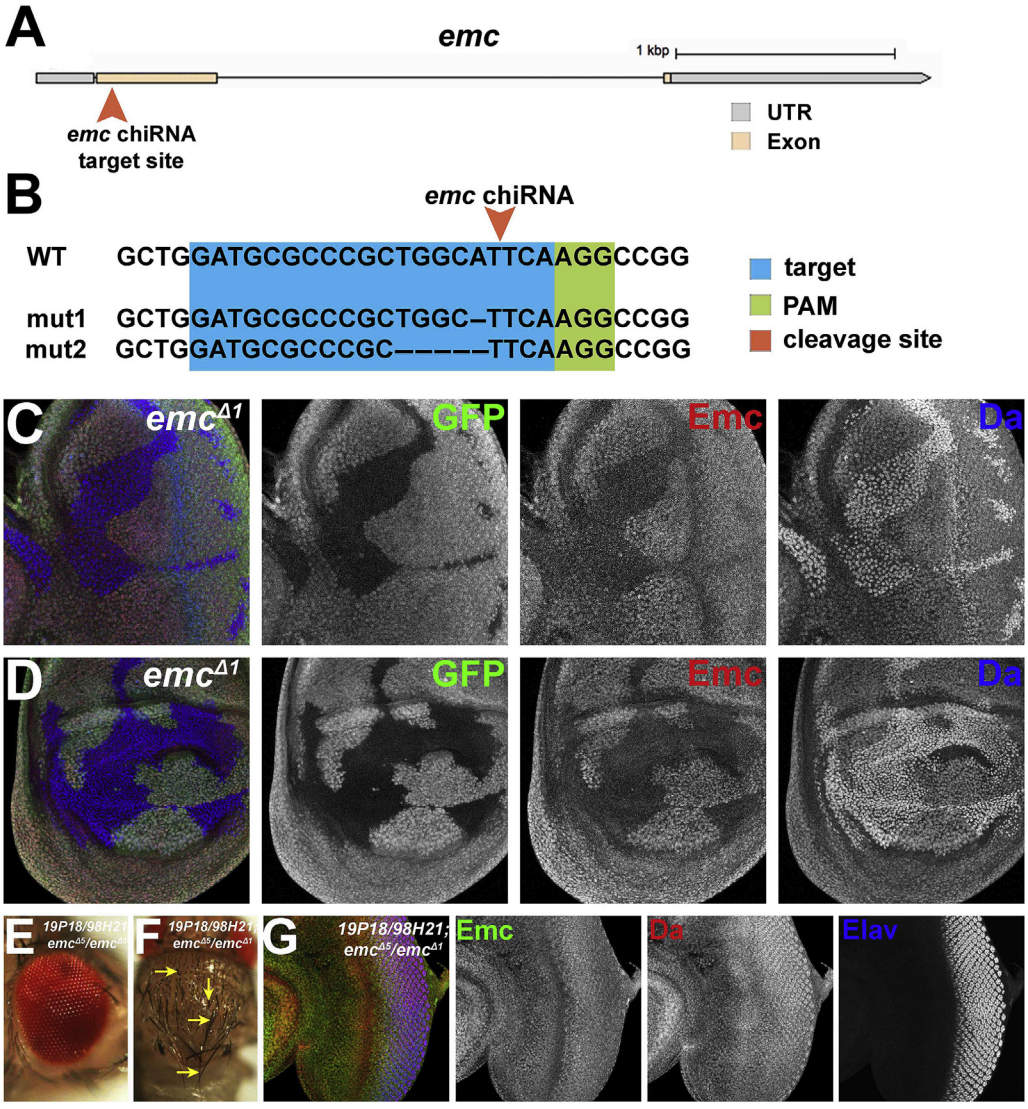

Fig. 2. Generation and validation of new mutant alleles of *emc*. (A) Schematic of the *emc* transcription unit showing the designed target site of the designed *emc* chiRNA. The target chiRNA is predicted to have no off-target and to cleave shortly after the transcription start site. (B) Comparing the sequencing results of two candidate *emc* amorphic mutants to the reference genome reveals successful deletions and frameshifts in both candidate alleles. emc^{mut1} has a one-bp deletion and therefore is named $emc^{\Delta 1}$, while emc^{mut2} has a five-bp deletion and therefore is named $emc^{\Delta 5}$. (C-D) Homozygous $emc^{\Delta 1}$ mutant clones are marked by the absence of GFP (green) in both developing eye (C) and wing (D) imaginal discs. $emc^{\Delta 1}$ mutant cells lack detectable Emc protein but upregulate Da consistent with previously reported characteristics of *emc* null alleles. These data strongly prove $emc^{\Delta 1}$ is a protein null mutation of *emc*. $emc^{\Delta 5}$ is indistinguishable from $emc^{\Delta 1}$ in all the assays performed and thus a second protein null allele of the *emc* gene. (E) The rescued pharate adult fly eyes appear morphologically normal. (F) The rescued adult flies have extra bristles (yellow arrows) on the thoraxes. (G) Emc and Da expression patterns appear largely normal in eye discs from the rescued larvae except the upregulation of Da normally seen in wild type morphogenetic furrow is less evident. All the photoreceptors differentiate normally as shown by Elav labeling. Genotypes: (C-D) *hsFLP;* $emc^{\Delta 1}$ *FRT80; Ubi-GFP M(3) 67C FRT80*, (E-G) *PBac{19P18, w+}/PBac{98H21,w+};* $emc^{\Delta 1}/emc^{\Delta 5}$.

the morphogenetic furrow that was more pronounced ventrally, delayed onset of Cut expression (a marker for cone cell development), and incorrect numbers of photoreceptor cells and cone cells per ommatidium (Figs. S2A and S2C). The results for $emc^{\Delta 5}$ were indistinguishable: the same higher Da, accelerated furrow progression, and defects in photoreceptor and cone cell patterning were observed. These results strongly suggested that $emc^{\Delta 1}$ and $emc^{\Delta 5}$ were genetic and protein null alleles of the *emc* gene.

We then combined the 19P18 and 98H21 genomic transgenes with $emc^{\Delta 1}/emc^{\Delta 5}$ transheterozygous mutants. The results were the same as when emc^{AP6} was rescued. At least one copy of either 19P18 or 98H21 was required to rescue the embryonic lethality of the *emc* mutants, all the rescued flies failed to eclose, and all the rescued pharate adults had the extra thoracic bristle phenotype (Fig. 2E–G). Altogether, these results suggested the pharate adult lethality and bristle phenotype most likely reflected insufficient *emc* function due to essential regulatory elements missing from both 19P18 and 98H21 genomic transgenes, rather than linked mutations in the other genes in the emc^{AP6} strain. In particular, it seems unlikely that $emc^{\Delta 1}$ or $emc^{\Delta 5}$ affects function of the *hng3* gene predicted on the opposite strand from *emc*, since these mutations deleted only 1bp and 5bp within the long alternative first intron of this gene. A P-element insertion 7bp upstream of the splice acceptor site for this intron does not affect adult viability or bristle patterning in the genotype $hng3^{5\text{-}SZ-3251}/Df$ (data not shown, Fig. 1A). Taken together, these data strongly suggest that the unique regions of BAC clones 19P18 and 98H21 must each contain redundant regulatory elements of the *emc* sufficient for survival to the pharate adult stage and for normal adult eye development. Other regulatory sequences required for normal patterning of thoracic bristles must be farther away from the *emc* transcription unit.

2.3. Da locally regulates emc transcription

A previous study concluded that Da regulated *emc* transcription. The evidence was that Emc protein was lost in *da* mutant clones and that *emc* transcript levels increased when Da was overexpressed (Bhattacharya and Baker, 2011). More recent results indicate that substantial *emc* can be supplied by uniform transcription, and that Da also regulates *emc* function at the level of protein stability (Li and Baker, 2018). Here we revisit the transcriptional regulation of *emc*, since while the original evidence argued that Da overexpression was sufficient to elevate *emc* transcription, this did not necessarily prove that *da* was required for *emc* transcription in normal development.

We used two methods to assay *emc* transcription, immunofluorescent in situ hybridization using antisense RNA probes to detect *emc* mRNA, and three different enhancer trap lines each inserted just upstream of the *emc* transcription start site, $emc\text{-}GFP^{YB0040}$, $emc\text{-}GFP^{YB0067}$ and *emc-LacZ*. Both in situ hybridization and enhancer traps revealed very similar *emc* transcription patterns to one another in the wing and eye discs that were also consistent with previous reports (Cubas and Modolell, 1992; Baonza et al., 2000; Baonza and Freeman, 2001; Bhattacharya and Baker, 2009; Spratford and Kumar, 2015). *emc* mRNA strongly accumulated in the equatorial region of the anterior eye disc but was sharply reduced in the morphogenetic furrow (Fig. 3A and Fig. S3A). The enhancers trap lines showed similar patterns to mRNA except that the reduced expression in the morphogenetic furrow extended up to column 2–3 more posteriorly, perhaps indicating greater stability of the enhancer trap reporter proteins (Bhattacharya and Baker, 2009) (Fig. 3C, Fig. S3C and E). Elevated equatorial enhancer trap expression anterior to the morphogenetic furrow is a response to Notch signaling (Bhattacharya and Baker, 2009; Spratford and Kumar, 2015). The pattern was still more complex in wing imaginal discs (Fig. 3B and D, Fig. S3B, D and F). For example, enhancer trap expression was maximal along the dorsal-ventral boundary of the wing margin but down-regulated in the proneural cells that flank this boundary in the anterior wing, all as reported previously (Cubas and Modolell, 1992; Baonza et al., 2000).

Fluorescent in situ hybridization was also performed in eye and wing imaginal discs containing *da* mutant clones. Little *emc* mRNA was observed in *da* mutant clones in a region of the eye disc, extending from just anterior to the morphogenetic furrow to the posterior of the eye disc, but no effect on *emc* RNA accumulation was seen in *da* mutant clones further anterior to the morphogenetic furrow (Fig. 3E and F). In wing imaginal discs, *emc* mRNA sometimes appeared lowered in *da* mutant cells, but often no change was detectable, regardless of location (Fig. 3G and H). Enhancer trap expression was also reduced in *da* mutant clones posterior to the furrow in the eye discs (Fig. 3I and Fig. S3G) but was not affected in any region in wing imaginal discs (Fig. 3J). Taken together, these data confirm that *da* is required for *emc* transcription, as concluded previously (Bhattacharya and Baker, 2011), but in only some imaginal disc regions. This contrasts with the apparently universal requirement for *da* function for Emc protein accumulation (Figs. S3H–I), which may depend largely on stabilization of Emc proteins (Bhattacharya and Baker, 2011; Li and Baker, 2018).

High and uniform Da levels are seen in *emc* mutant cells. To determine how much of that effect is attributed to transcriptional upregulation of *da* expression, we examined activities of a previously described *da* enhancer in *emc* mutant cells using a transgenic reporter. While Da protein is highly upregulated in *emc* mutants in all tissues examined so far (Bhattacharya and Baker, 2011) (Fig. 3K-L), *da* enhancer activity was upregulated modestly in *emc* mutant cells in wing discs but not detectably in eye discs. These results supported the previous conclusion that Emc suppresses Da-dependent *da* transcription, at least in wing discs. The failure to detect an effect in eye discs suggests that Emc might depress Da protein levels post-transcriptionally, such as through the effect of Emc on Da protein stability that was seen in transfected tissue culture cells (Li and Baker, 2018).

2.4. Emc transcription is regulated in proneural regions

Emc protein is downregulated in proneural regions, including the morphogenetic furrow of the eye disc and the anterior margin of the wing disc. In the morphogenetic furrow, Dpp and Hh signaling synergistically reduce Emc protein (Bhattacharya and Baker, 2011). The proneural gene *atonal* is also required for reducing Emc protein in the morphogenetic furrow, but this does not explain the parallel loss of *emc* mRNA (Li and Baker, 2018). Since transcription of *ato* depends on the Dpp and Hh pathways (Greenwood and Struhl, 1999; Curtiss and Mlodzik, 2000), we tested if Dpp and Hh signaling also repress *emc* transcription, using *smo Mad* double mutant cells that are unable to respond to Hh or Dpp. Emc enhancer trap expression was de-repressed in *smo Mad* mutant cells in the morphogenetic furrow (Fig. 4A), suggesting that Hh or Dpp indeed repress *emc* transcription. *emc-GFP* reporter was seemingly lower in *smo Mad* mutant cells posterior to the morphogenetic furrow.

Emc protein is down-regulated at the anterior wing margin by proneural proteins from the AS-C, but it is not known how *emc* mRNA is regulated there. It has been suggested Wg signaling is responsible for patterning the wing margin. Wg is expressed along the presumptive wing margin during the third instar larva and contributes to AS-C expression there (Couso et al., 1994). Wg is also necessary and sufficient for the expression of Sens (Jafar-Nejad et al., 2006). We found that Emc protein levels were no longer reduced in wing margin cells mutant for the Wg co-receptor *arrow (arr)* or for the Wg target gene *sens* (Fig. 4B and C). Thus, Wg signaling, directly or through its more downstream effectors AS-C and Sens, might contribute to *emc* mRNA regulation at the anterior wing margin.

2.5. Post-transcriptional regulation of emc is independent of the miRNA machinery

In addition to protein stability, another way that Emc protein levels could be regulated after uniform transcription is through 3′ UTR sequences, for example by miRNAs. Interestingly, the gain-of-function allele emc^{D} is associated with insertion of a 5.7 kb transposon that,

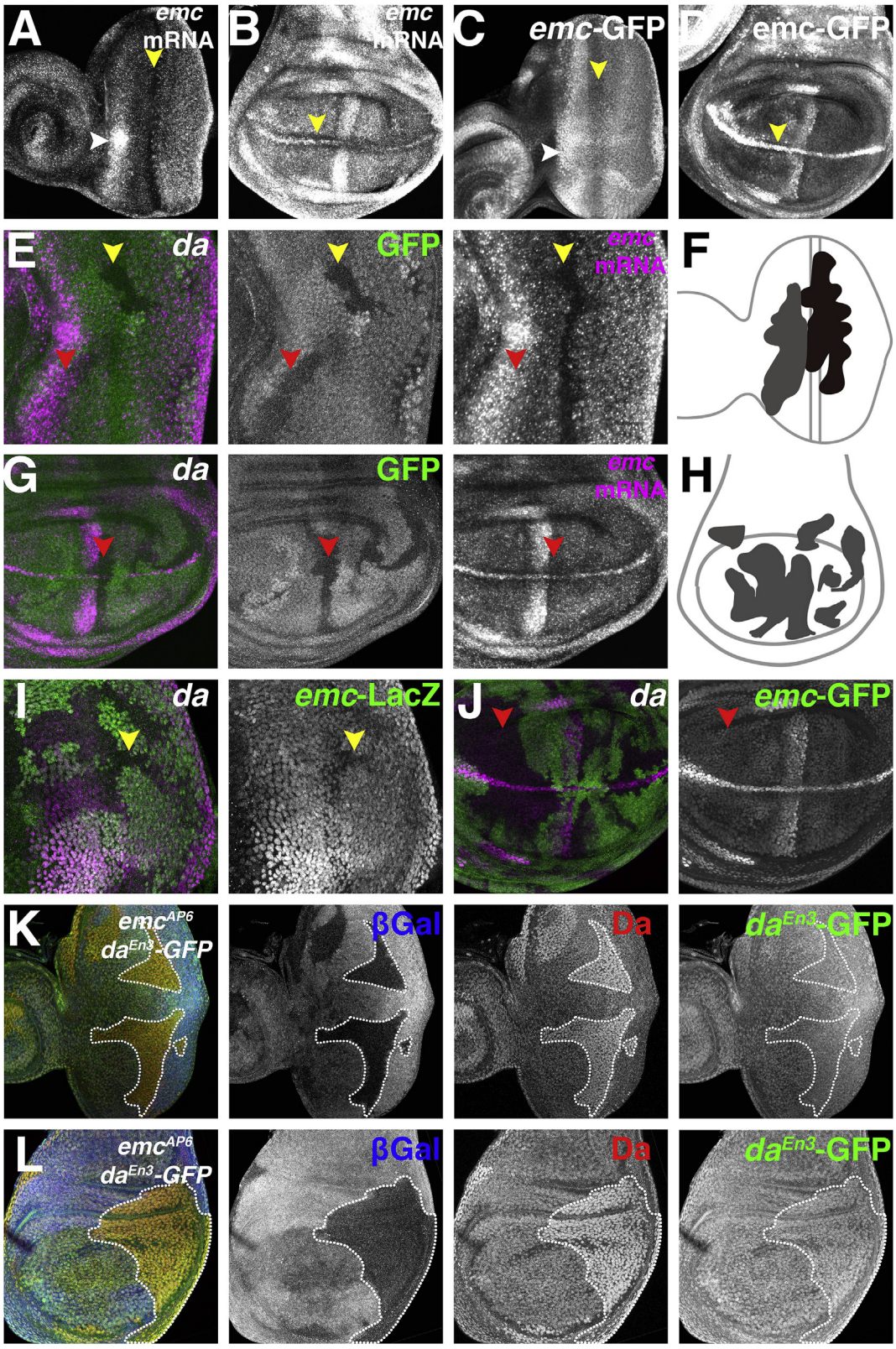

(caption on next page)

Fig. 3. Transcriptional regulation of *emc* and *da*. (A) Fluorescent in situ hybridization detected *emc* mRNA in wild type developing eye imaginal discs, showing accumulation at the anterior equatorial region (white arrowhead) and downregulation in the furrow (yellow arrowhead). (B) *emc* mRNA is detected in a pattern in the wild type wing disc that includes downregulation in the proneural regions at the wing margin (yellow arrowhead). (C) *emc* enhancer trap expression in the eye disc in the *emc-GFP*^{YB0067} line, showing a broader downregulation stripe near the furrow (yellow arrowhead) and a similar accumulation at the anterior equatorial region (white arrowhead) compared to *emc* mRNA pattern. (D) *emc* enhancer trap expression in the wing disc in the *emc-GFP*^{YB0067} line showing downregulation in the proneural regions at the wing margin (yellow arrowhead). (E–L) Homozygous *da* or *emc* mutant clones are marked by the absence of GFP or βGal. (E) *emc* mRNA (magenta) is downregulated in *da* clones in eye disc in regions that are close to the furrow (yellow arrowhead). However, *emc* transcription is not affected in *da* clones that are further anterior to the furrow (red arrowhead). (F) Map of eye imaginal disc showing regions where *emc* transcription is dependent on Da (black) and where it is not (grey). (G) *emc* mRNA (magenta) remains unchanged in *da* clones in wing disc (red arrowhead). (H) Map of wing imaginal disc showing *emc* transcription is not dependent on Da in the wing (grey). (I) In eye discs, *emc* enhancer trap expression (magenta) is reduced in *da* clones posterior to the furrow (yellow arrowhead) but remains unchanged in *da* clones anterior to the furrow. (J) *emc* enhancer trap expression (magenta) remains unaffected in *da* clones in wing discs (red arrowhead). (K) *da* enhancer reporter (green) remains unchanged in *emc* mutant cells (marked by dashed lines) in eye discs while Da protein (red) is significantly upregulated. (L) Both *da* reporter and Da protein are upregulated in *emc* mutant cells in (marked by dashed lines) wing discs, although the effect on the reporter is more modest. Genotypes: (A–B) *w*^{1118}, (C–D) *emc-GFP*^{YB0067}/+, (E, G) *hsFLP; da*^{3} *FRT40/Ubi-GFP FRT40*, (I) *eyFLP; da*^{3} *FRT40/Ubi-GFP FRT40; P{PZ}emc*^{04322}/+, (J) *UbxFLP; da*^{3} *FRT40/arm-LacZ FRT40; emc-GFP*^{YB0040}/+, (K–L) *hsFLP; da*^{En3}*-GFP/+; emc*^{AP6} *FRT80/arm-lacZ M(3)67C FRT80.*

although not directly assessed, is expected to interfere with 3′ UTR transcription and truncate the wild type protein (Garrell and Modolell, 1990) (Fig. 1B). In situ hybridization showed that while the general patterns were similar in wild type and *emc*^{D} discs, the overall levels of *emc* transcripts were clearly higher in the *emc*^{D} background (Figs. S4A–D) (Cubas and Modolell, 1992). The overall patterns of *emc* mRNAs are more heterogeneous than that of the protein especially in the wing imaginal discs, suggesting *emc* mRNA might undergo post-transcriptional regulation through its 3′UTR (Fig. 1D, Figs. S1A, S4A and C). We could not assess the effect of *emc*^{D} on Emc protein levels directly, because the Emc^{D} protein was not recognized by the available Emc antibody (Fig. S4E). We noted, however, that *emc*^{D}/+ cells exhibited roughly half the antibody labeling of wild type cells, which would be consistent with similar protein expression levels from the *emc*^{D} and wild type alleles (Fig. S4E). This is consistent with the fact that Da expression remained unchanged in homozygous *emc*^{D} cells, especially in the morphogenetic furrow where Da level is sensitive to high levels of Emc (Fig. S4F). In our hands the *emc*^{D} mutation no longer exhibits much dominant phenotype in *emc*^{D}/+ flies, but *emc*^{D}/*emc*^{D} homozygotes lack many macro- and micro-chaetae, as described previously (data not shown).

We next assessed the contribution of miRNAs to Emc protein levels using previously established approaches. We examined cells that were homozygously mutant for both *dcr1* and *pasha*^{KO}, two core components of the miRNA biogenesis pathway (Martin et al., 2009). These mutations did not affect Emc protein levels. Specifically, the downregulation of Emc protein in the morphogenetic furrow in the eye disc and anterior wing margin in the wing disc remained in *dcr1 pasha*^{KO} mutant clones. (Fig. 5A and B). Similar results were obtained when Gal4-mediated *gw* RNAi expression was driven in clones to silence the miRNA pathway (Smibert et al., 2013). No discernible effects on Emc protein level were observed when *gw* was silenced (Fig. 5C and D). Although these results do not rule out any effect of miRNAs on *emc* mRNA accumulation, they do indicate that any such regulation is unlikely to be required for the normal levels of Emc protein, and therefore not important for the rescue of *emc* mutant phenotypes by uniform transcription.

3. Discussion

Since the *emc* gene shows complex transcriptional regulation, it was surprising to find that *emc* null mutants can be substantially rescued by uniform *emc* transcription (Li and Baker, 2018). In this paper, we re-examined regulation of *emc* transcription in light of recent discoveries. Our data suggest that both upstream and downstream *cis*-regulatory elements are important for *emc* transcription, and that some regulatory elements must be outside a 35 kb region surrounding the transcription unit. Although we did find that Da is required for *emc* transcription, this was only in certain tissues, whereas the role of Da in stabilizing Emc protein is more general. In addition to the known roles of Notch signaling

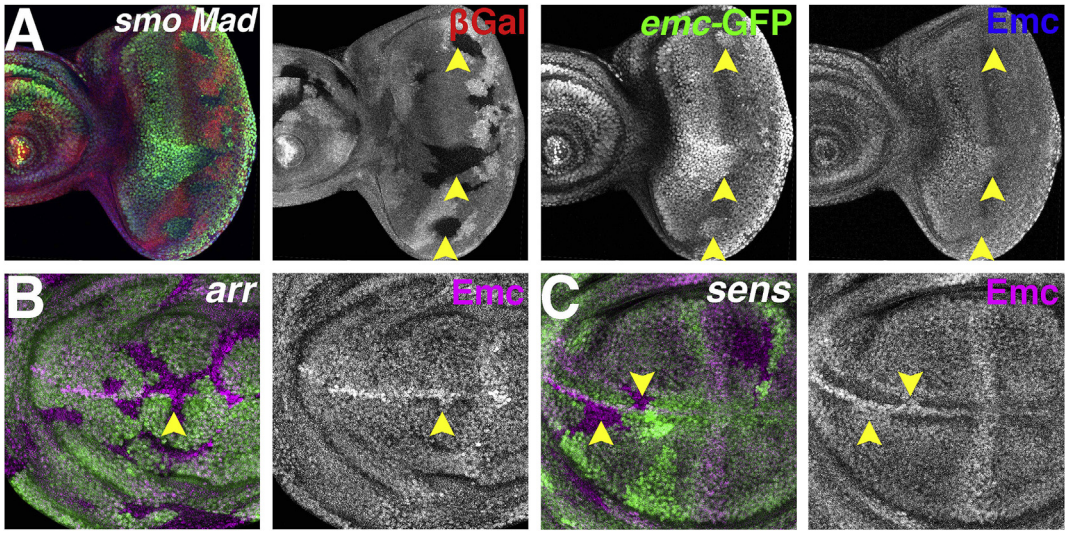

Fig. 4. Repression of Emc expression by signaling pathways. Homozygous mutant clones are marked by the absence of βGal (A, red) or GFP (B and C, green). (A) *emc-GFP* is no longer downregulation in *smo Mad* clones in the furrow. In *smo Mad* clones anterior to the furrow (yellow arrowheads), *emc-GFP* appears to be upregulated, whereas in those posterior to the furrow, *emc-GFP* is autonomously downregulated but maintained near the clone boundaries. Emc protein (blue) is maintained in the clones in the furrow as previously reported. (B) Emc (magenta) is no longer downregulated in cells lacking *arr* which do not respond to Wg signaling. (C) Emc (magenta) is retained in cells lacking *sens* in the wing margin of the wing discs. Genotypes: (A) *hsFLP; smo*^{Q14}*, Mad*$^{1-2}$ *FRT40/arm-lacZ FRT40, emc-GFP*^{YB0040}/+, (B) *hsFLP; FRT42 arr*^{2}*/FRT42 M(2)56F Ubi-GFP*, (C) *hsFLP; sens*^{E2} *FRT80/Ubi-GFP FRT80.*

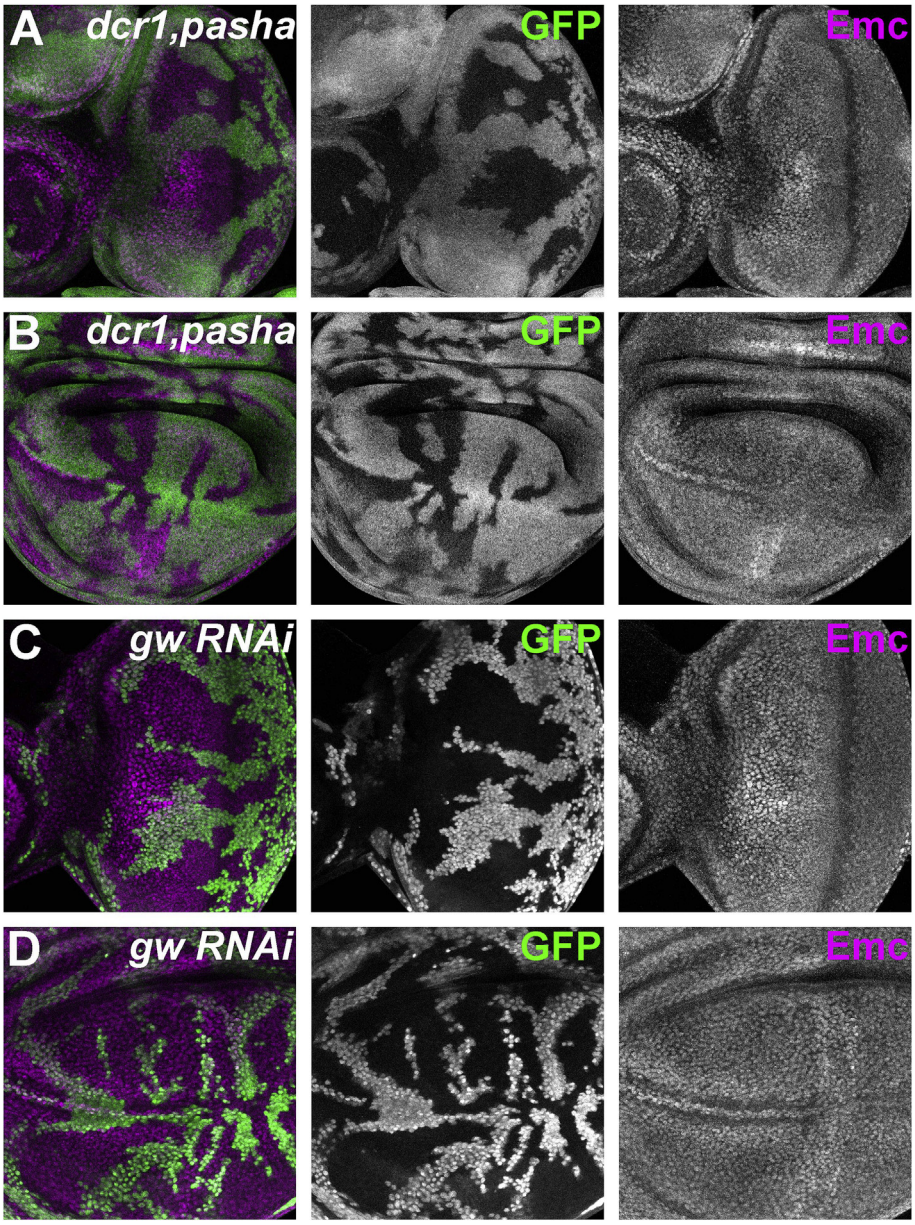

Fig. 5. MiRNA pathways and Emc expression. (A–B) Homozygous *dcr1 pasha* double mutant clones are marked by the absence of GFP (green). (A) In eye discs, *dcr1 pasha* double mutant cells show normal Emc protein expression. (B) In wing discs, Emc protein expression remains unchanged in *dcr1 pasha* double mutant cells. (C–D) Flip-on clones expressing *gw RNAi* using *act-Gal4* are positively marked by GFP (green). Knocking down *gw* functions has little effect on Emc expression in eye (C) and wing (D) discs. Genotypes: (A–B) *hsFLP; FRT82 dcr1*^{Q1147X} *pasha*^{KO}*/FRT82 Ubi-GFP M(3)95A*, (C–D) *hsFLP; UAS-gw RNAi/+; act > CD2>Gal4, UAS-GFP/+*.

in *emc* transcriptional regulation, we demonstrated that Hh, Dpp and perhaps Wg signaling affected *emc* transcription in particular tissues. Despite this elaborate transcriptional regulation, as well as possibly post-transcriptional regulation of mRNA stability and translation, all our data were consistent with the Emc protein levels being determined mostly at the post-translational level. This suggests that prepatterns for neural development in *Drosophila* may be defined by post-transcriptional mechanisms at least as much as by transcriptional regulation.

Because the existing null allele *emc*^{AP6} was never completely rescued by genomic transgenes together encompassing 35 kb of genomic DNA, we made two new molecularly-defined null alleles, *emc*$^{\Delta 1}$ and *emc*$^{\Delta 5}$. These had similar phenotypes to *emc*^{AP6} but were less likely to affect other genes. Our studies indicated that *emc* function depended on transcriptional regulatory sequences mapping within the 15 kb upstream of the *emc* transcription unit and within the 11 kb downstream, and that these regions are required redundantly. Some essential sequences must map still further from the *emc* transcription unit, because even combining multiple regulatory regions did not rescue *emc* function completely, and in the case of the new *emc*$^{\Delta 1}$ and *emc*$^{\Delta 5}$ alleles this was unlikely to indicate disruption of the *hng3* gene predicted on the opposite strand, or of other linked genes. Although Janelia Gal4 lines mapped four regions close to *emc* capable of driving transcription in specific neural cells (Jory et al., 2012; Spratford and Kumar, 2015), only two of these map close to the transcription unit, within a 10 kb region that is not able to rescue significant *emc* function.

Interestingly, in these and previous studies where we have transcribed *emc* from different transgenic sources at distinct levels, adult eye development has been normal whereas level-dependent developmental defects have been seen in the thoracic bristle patterning (Bhattacharya and Baker, 2011; Li and Baker, 2018). This suggests different proneural regions in *Drosophila* have different sensitivities to Emc function.

One gene that is required for *emc* function is *da*, so that the phenotypes of *da* and of *da emc* null clones are indistinguishable (Bhattacharya and Baker, 2011). Da is a transcription factor and its association with multiple regions around the *emc* locus was previously reported in a chromatin immunoprecipitation (ChIP)-chip database of early *Drosophila* embryos (MacArthur et al., 2009). Nevertheless, we only found evidence that *da* was required for *emc* transcription in the eye disc posterior to the

morphogenetic furrow. The more general role for Da may be in stabilizing Emc proteins. In the wing disc especially, *emc* transcripts and enhancer traps show complex patterns of transcription that are less evident at the level of Emc protein (and not reflected in the Da expression pattern), further indicating that Emc protein levels are predominantly regulated post-transcriptionally. In the eye disc, *emc* transcription is elevated in the equatorial region by Notch signaling but this is less evident in the Emc protein and apparently not functionally important, since eye development is rescued by uniform *emc* transcription whereupon Emc protein is not upregulated in this region. Even the requirement demonstrated for *da* for *emc* transcription in the eye disc might not be direct. Since *da* mutant cells lack most eye differentiation (Brown et al., 1996), they could affect *emc* transcription indirectly. *Emc* transcription in the eye disc posterior to the furrow also depended on Ato, the heterodimer partner of Da, but since Ato is mainly expressed in R8 photoreceptor precursors, it presumably affects *emc* transcription in non-R8 cells indirectly (Li and Baker, 2018).

Our results suggested extracellular signaling pathways reduce Emc expression in several ways. Dpp and Hh downregulate Emc in the morphogenetic furrow, which parallels the their role in inducing Ato expression (Greenwood and Struhl, 1999; Curtiss and Mlodzik, 2000; Bhattacharya and Baker, 2011). Ato destabilizes Emc protein, but is not responsible for transcriptionally repressing *emc* in the furrow (Li and Baker, 2018). Here we found that Dpp or Hh signaling pathways repressed *emc* transcription in the morphogenetic furrow in the eye. In cells that do not respond to Dpp or Hh pathways, both *emc* transcription and Emc protein were retained, which suggested Dpp or Hh repress *emc* transcription independent of Ato. At the anterior wing margin, loss of Emc protein depended on Wg signaling and on Sens expression, although we do not know whether this is independent of the requirement for AS-C that was already described (Li and Baker, 2018) or whether the effect is transcriptional. Interestingly, Sens was previously found to physically interact with Da (Jafar-Nejad et al., 2006), a primary stabilizer of Emc protein, and therefore may also destabilizes Emc by competitively binding to Da in the anterior wing margin.

The 3′ UTR could be involved in regulating *emc* mRNA levels. The *emc* 3′UTR contains one Brd box and four GY box-related motifs, which are known to be involved in destabilizing mRNA (Lai and Posakony, 1997; Leviten et al., 1997). Two neuronal RNA binding proteins from the Elav/Hu protein family were previously reported to bind to *emc/ID* mRNAs. The Rbp9 protein binds to the *emc* 3′ UTR and destabilizes it, but the *Rbp9* mutant lacks any bristle or eye phenotype (Park et al., 1998; Zaharieva et al., 2015). Hel-N1, a human homolog of the *Drosophila elav* gene, binds to 3′ UTR of mRNA for ID genes, and the binding sequences are conserved in the *emc* gene (King et al., 1994). We have also found that Emc protein levels were unchanged in cells depleted of *dcr1* and *pasha* or of *gw*, functions that are essential for miRNA biogenesis or function. An emc^{D} allele exists that is unlikely to encode the normal 3′ UTR sequences. The elevated mRNA levels observed in emc^{D} might also reflect transcriptional changes. The elevated mRNA levels lack visible effects on $emc^{D}/+$ flies, however, and although we could not measure Emc^{D} protein levels directly, if they were greatly elevated then we would expect to see a corresponding reduction in wild type protein, which was not observed. It is possible that Emc protein levels exceed the phenotypic threshold in emc^{D}/emc^{D} flies. Alternatively, the possibility cannot be excluded that it is changes in the Emc^{D} protein sequence that are responsible for the emc^{D} mutant phenotype.

Our results suggest that, despite multiple pathways that impact *emc* mRNA levels, within certain bounds Emc protein levels are largely determined by stability, which may be a more important consideration than transcriptional regulation. This suggests that post-translational mechanisms, such as the heterodimer interactions with Emc partner proteins (Li and Baker, 2018), or the modification of proneural bHLH proteins themselves (Baker and Brown, 2018), may be key aspects of the proneural prepattern, and might also be important for neuronal reprogramming strategies in mammals (Guillemot and Hassan, 2017; Jorstad et al., 2017).

The *emc* gene has four homologs (ID1-4) in mammals. High levels of ID proteins expression have been reported in almost all types cancer and they are thought to contribute to many cancer-related properties (Perk et al., 2005; Lasorella et al., 2014). ID proteins and E proteins are also associated with many neurocognitive disorders (Wang and Baker, 2015). As in *Drosophila*, many mammalian studies have also focused on signaling pathways that activate *ID* gene transcription, including multiple oncogenic pathways (MYC, RAS, SRC etc.) and growth factor signals (FGF, BMP etc.). This supports the idea of targeting ID protein interactions with other proteins as a therapeutic approach for cancer and other diseases (Lasorella et al., 2014).

4. Methods and materials

4.1. Drosophila stocks

The following stocks were employed in this study and strains were maintained at 25 °C unless otherwise stated. da^{3} (Cronmiller and Cline, 1987), emc^{AP6} (Ellis, 1994), emc-GFP^{YB0040} and emc-GFP^{YB0067} (Quinones-Coello et al., 2007), P{PZ}emc^{04322} (Rottgen et al., 1998), smo^{Q14}, Mad^{1-2}, $dcr1^{Q1147X}$ (Lee et al., 2004), $pasha^{KO}$ (Martin et al., 2009), *(3L)ED202*, *Df(3L)ED207* and *Df(3L)ED4177* (used interchangeably as deletions including the *emc* locus, with equivalent results), *Ubi-GFP M(3)67C FRT80*, *FRT42 M(2)56F Ubi-GFP*, *FRT82 M(3)95A Ubi-GFP*.

4.2. Mosaic analysis

Mosaic clones were obtained using FLP/FRT mediated mitotic recombination. To make clones induced by hsFLP, non-Minute larvae were subjected to heat shock for 1 h at 37 °C at 60 ± 12 h after egg laying whereas Minute larvae were heat shocked at 84 ± 12 h after egg laying. Wandering third-instar larvae were dissected 72 h after heat shock.

4.3. Constructs for transgenesis

To make transgenic flies carrying the BACs, corresponding BAC clone vectors were inserted at 59D3 (chromosome 2R) using PhiC31-mediated site-specific integration. To make the 10 kb-transgenic flies, a 5.3 kb fragment from the 19P18 BAC clone and a 4.7 kb fragment from the 98H21 BAC clone were cloned into pBlueScript KS(−) before transfer into the pattB vector. The resulting pattB-10kb construct was also inserted at 59D3 (2R) using site-specific integration. To make the *da* enhancer reporter flies, the same construct used in our previous study (Bhattacharya and Baker, 2011) was re-injected to integrate on the 2nd chromosome via site-directed mutagenesis. Whereas the original insertion at 68A4 was subject to position-effect variegation, this was not seen with the insert at 55C4.

4.4. CRISPR/Cas9-mediated emc mutagenesis

Cas9 target sequence was predicted and selected using flyCRISPR Optimal Target Finder (http://tools.flycrispr.molbio.wisc.edu/targetFinder/). One target predicted to have no off-target and expected to introduce small indels upstream of the HLH domain was selected (5′-CCTTGAATGCCAGCGGGCGCATC with PAM target site underlined). Sense oligo (5′-CTTCGATGCGCCCGCTGGCATTCA) and antisense oligo (5′-AAACTGAATGCCAGCGGGCGCATC) were annealed, digested and ligated into the pU6-*Bbs*I-chiRNA vector to generate pU6-*Bbs*I-chiRNA*emc*. Vector was injected at the concentration of 250ng/ul and 125ng/ul into fly embryos that express germline Cas9 by Bestgene. Founders were crossed individually to *TM2,* emc^{1} balancer flies. Candidate mutations selected by non-complementation with emc^{1} were confirmed by Sanger sequencing of the *emc* locus.

4.5. Immunohistochemistry and image processing

Antibody staining was performed as previously described (Baker et al., 2014). The following primary antibodies were used: mouse anti-βGal (1:100, DSHB 40-1a), rat anti-Elav (1:50, DSHB 7E8A10), mouse anti-Da (1:200), rabbit anti-Emc (1:8000, a gift from Y. N. Jan), rat anti-GFP (1:1000, Nacalai Tesque GF090R), guinea pig anti-Sens. Secondary antibodies conjugated with Cy2, Cy3 and Cy5 dyes (1:200) were from Jackson ImmunoResearch Laboratories. Multi-labeled samples were sequentially scanned with Leica SP2 or SP5 confocal microscopes. Z-stacks were projected using Max Intensity and processed with ImageJ. At least six samples were analyzed for each genotype.

4.6. RNA in situ hybridization and simultaneous detection of RNA and protein

Probe preparation and detection were performed as previously described (Firth and Baker, 2007). Two RNA probes between 500 and 600 base pairs were designed against unique sequences of the *emc* cDNA, with equivalent results. Sequence-specific primers used for the second PCR reactions are: *emc*-FISH1-5′ GGCCGCGGAATCCGGTACGACCGTGTAA, *emc*-FISH1-3′ CCCGGGGCGCTGCTGTGATTGCAGTTGT, *emc*-FISH2-5′ GGCCGCGGGCACAAAGCCGAAATCAAAT, *emc*-FISH2-3′ CCCGGGGCGC-GAGGATATCTGGATCGAC. Simultaneous detection of RNA and protein were performed as previously described (Baker et al., 2014). Briefly, tissue was prepared and processed as discussed above. Primary antibody against GFP (which marks our clones) was added simultaneously with the HRP-conjugated antibody against the hybridized RNA probe. Cy2-conjugated secondary antibody was used to label the GFP signal, followed by the developmental and TSA amplification of the in situ signal. Image were acquired and processed as described above. At least 10 samples were analyzed for Fig. 3E–H.

Acknowledgement

We thank Drs. E. Lai and Y. N. Jan for reagents and S. Nair and V. Reddy for comments. Drosophila stocks were obtained from the Flytrap Project and the Bloomington Drosophila Stock Center (supported by NIH P40OD018537). We thanks Flybase for the genome browser display of the *emc* locus. Confocal microscopy was performed in the Analytical Imaging Facility of the Albert Einstein College of Medicine (supported by the NCI P30CA013330). DNA sequencing was performed by the Genomics Core of Albert Einstein College of Medicine. This work was supported by the NIH grant GM047892. Data in this paper are from a thesis submitted in partial fulfillment of the requirement for the degree of Doctor of Philosophy in the Graduate Division of Biomedical Sciences, Albert Einstein College of Medicine, Yeshiva University, USA.

Appendix A. Supplementary data

Supplementary data to this article can be found online at https://doi.org/10.1016/j.ydbio.2019.02.003.

References

Adam, J.C., Montell, D.J., 2004. A role for extra macrochaetae downstream of Notch in follicle cell differentiation. Development 131, 5971–5980.
Baker, N.E., Brown, N.L., 2018. All in the family: neuronal diversity and proneural bHLH genes. Development 145 dev159426.
Baker, N.E., Li, K., Quiquand, M., Ruggiero, R., Wang, L.H., 2014. Eye development. Methods 68, 252–259.
Baonza, A., Freeman, M., 2001. Notch signalling and the initiation of neural development in the Drosophila eye. Development 128, 3889–3898.
Baonza, A., de Celis, J.F., Garcia-Bellido, A., 2000. Relationships between extramacrochaetae and Notch signalling in Drosophila wing development. Development 127, 2383–2393.
Benezra, R., Davis, R.L., Lockshon, D., Turner, D.L., Weintraub, H., 1990. The protein Id: a negative regulator of helix-loop-helix DNA binding proteins. Cell 61, 49–59.
Bhattacharya, A., Baker, N.E., 2009. The HLH protein Extramacrochaetae is required for R7 cell and cone cell fates in the *Drosophila* eye. Dev. Biol. 327, 288–300.
Bhattacharya, A., Baker, N.E., 2011. A network of broadly expressed HLH genes regulates tissue-specific cell fates. Cell 147, 881–892.
Botas, J., Moscoso del Prado, J., Garcia-Bellido, A., 1982. Gene-dose titration analysis in the search of trans-regulatory genes in *Drosophila*. EMBO J. 1, 307–310.
Brown, N.L., Sattler, C.A., Paddock, S.W., Carroll, S.B., 1995. Hairy and emc negatively regulate morphogenetic furrow progression in the drosophila eye. Cell 80, 879–887.
Brown, N.L., Paddock, S.W., Sattler, C.A., Cronmiller, C., Thomas, B.J., Carroll, S.B., 1996. *Daughterless* is required for *Drosophila* photoreceptor cell determination, eye morphogenesis, and cell cycle progression. Dev. Biol. 179, 65–78.
Couso, J.P., Bishop, S.A., Martinez Arias, A., 1994. The wingless signalling pathway and the patterning of the wing margin in Drosophila. Development 120, 621–636.
Cronmiller, C., Cline, T.W., 1987. The Drosophila sex determination gene daughterless has different functions in the germ line versus the soma. Cell 48, 479–487.
Cubas, P., Modolell, J., 1992. The *extramacrochaetae* gene provides information for sensory organ patterning. EMBO J. 11, 3385–3393.
Curtiss, J., Mlodzik, M., 2000. Morphogenetic furrow initiation and progression during eye development in Drosophila: the roles of decapentaplegic, hedgehog and eyes absent. Development 127, 1325–1336.
Ellis, H.M., 1994. Embryonic expression and function of the Drosophila helix-loop-helix gene, extramacrochaetae. Mech. Dev. 47, 65–72.
Ellis, H.M., Spann, D.R., Posakony, J.W., 1990. *extramacrochaetae*, a negative regulator of sensory organ development in *Drosophila*, defines a new class of helix-loop-helix proteins. Cell 61, 27–38.
Firth, L.C., Baker, N.E., 2007. Spitz from the retina regulates genes transcribed in the second mitotic wave, peripodial epithelium, glia and plasmatocytes of the *Drosophila* eye imaginal disc. Dev. Biol. 307, 521–538.
Garrell, J., Modolell, J., 1990. The Drosophila extramacrochaetae locus, an antagonist of proneural genes that, like these genes, encodes a helix-loop-helix protein. Cell 61, 39–48.
Greenwood, S., Struhl, G., 1999. Progression of the morphogenetic furrow in the Drosophila eye: the roles of Hedgehog, Decapentaplegic and the Raf pathway. Development 126, 5795–5808.
Guillemot, F., Hassan, B.A., 2017. Beyond proneural: emerging functions and regulations of proneural proteins. Curr. Opin. Neurobiol. 42, 93–101.
Jafar-Nejad, H., Tien, A.C., Acar, M., Bellen, H.J., 2006. Senseless and Daughterless confer neuronal identity to epithelial cells in the Drosophila wing margin. Development 133, 1683–1692.
Jorstad, N.L., Wilken, M.S., Grimes, W.N., Wohl, S.G., VandenBosch, L.S., Yoshimatsu, T., Wong, R.O., Rieke, F., Reh, T.A., 2017. Stimulation of functional neuronal regeneration from Muller glia in adult mice. Nature 548, 103–107.
Jory, A., Estella, C., Giorgianni, M.W., Slattery, M., Laverty, T.R., Rubin, G.M., Mann, R.S., 2012. A survey of 6,300 genomic fragments for cis-regulatory activity in the imaginal discs of Drosophila melanogaster. Cell Rep. 2, 1014–1024.
King, P.H., Levine, T.D., Fremeau Jr., R.T., Keene, J.D., 1994. Mammalian homologs of Drosophila ELAV localized to a neuronal subset can bind in vitro to the 3' UTR of mRNA encoding the Id transcriptional repressor. J. Neurosci. 14, 1943–1952.
Lai, E.C., Posakony, W., 1997. The bearded box, a novel 3 ' UTR sequence motif, mediates negative posttranscriptional regulation of bearded and enhancer of split complex gene expression. Development 124, 4847–4856.
Lasorella, A., Benezra, R., Iavarone, A., 2014. The ID proteins: master regulators of cancer stem cells and tumour aggressiveness. Nat. Rev. Cancer 14, 77–91.
Lee, Y.S., Nakahara, K., Pham, J.W., Kim, K., He, Z., Sontheimer, E.J., Carthew, R.W., 2004. Distinct roles for Drosophila Dicer-1 and Dicer-2 in the siRNA/miRNA silencing pathways. Cell 117, 69–81.
Leviten, M.W., Lai, E.C., Posakony, J.W., 1997. The Drosophila gene *bearded* encodes a novel small protein and shares 3' UTR sequence motifs with multiple enhancer of split complex genes. Development 124, 4039–4051.
Li, K., Baker, N.E., 2018. Regulation of the Drosophila ID protein Extra macrochaetae by proneural dimerization partners. Elife 7.
MacArthur, S., Li, X.Y., Li, J., Brown, J.B., Chu, H.C., Zeng, L., Grondona, B.P., Hechmer, A., Simirenko, L., Keranen, S.V., Knowles, D.W., Stapleton, M., Bickel, P., Biggin, M.D., Eisen, M.B., 2009. Developmental roles of 21 drosophila transcription factors are determined by quantitative differences in binding to an overlapping set of thousands of genomic regions. Genome Biol. 10, R80.
Martin, R., Smibert, P., Yalcin, A., Tyler, D.M., Schafer, U., Tuschl, T., Lai, E.C., 2009. A Drosophila pasha mutant distinguishes the canonical microRNA and mirtron pathways. Mol. Cell Biol. 29, 861–870.
Massari, M.E., Murre, C., 2000. Helix-loop-helix proteins: regulators of transcription in eukaryotic organisms. Mol. Cell Biol. 20, 429–440.
Murre, C., 2019. Helix-loop-helix proteins and the advent of cellular diversity: 30 years of discovery. Genes Dev. 33, 6–25.
Park, S.J., Yang, E.S., Kim-Ha, J., Kim, Y.J., 1998. Down regulation of extramacrochaetae mRNA by a Drosophila neural RNA binding protein Rbp9 which is homologous to human Hu proteins. Nucleic Acids Res. 26, 2989–2994.
Perk, J., Iavarone, A., Benezra, R., 2005. Id family of helix-loop-helix proteins in cancer. Nat. Rev. Cancer 5, 603–614.
Quinones-Coello, A.T., Petrella, L.N., Ayers, K., Melillo, A., Mazzalupo, S., Hudson, A.M., Wang, S., Castiblanco, C., Buszczak, M., Hoskins, R.A., Cooley, L., 2007. Exploring strategies for protein trapping in drosophila. Genetics 175, 1089–1104.
Rodriguez, I., Hernandez, R., Modolell, J., Ruiz-Gomez, M., 1990. Competence to develop sensory organs is temporally and spatially regulated in Drosophila epidermal primordia. EMBO J. 9, 3583–3592.
Rottgen, G., Wagner, T., Hinz, U., 1998. A genetic screen for elements of the network that regulates neurogenesis in Drosophila. Mol. Gen. Genet. 257, 442–451.

Schmitz, R., Young, R.M., Ceribelli, M., Jhavar, S., Xiao, W., Zhang, M., Wright, G., Shaffer, A.L., Hodson, D.J., Buras, E., Liu, X., Powell, J., Yang, Y., Xu, W., Zhao, H., Kohlhammer, H., Rosenwald, A., Kluin, P., Muller-Hermelink, H.K., Ott, G., Gascoyne, R.D., Connors, J.M., Rimsza, L.M., Campo, E., Jaffe, E.S., Delabie, J., Smeland, E.B., Ogwang, M.D., Reynolds, S.J., Fisher, R.I., Braziel, R.M., Tubbs, R.R., Cook, J.R., Weisenburger, D.D., Chan, W.C., Pittaluga, S., Wilson, W., Waldmann, T.A., Rowe, M., Mbulaiteye, S.M., Rickinson, A.B., Staudt, L.M., 2012. Burkitt lymphoma pathogenesis and therapeutic targets from structural and functional genomics. Nature 490, 116–120.

Smibert, P., Yang, J.S., Azzam, G., Liu, J.L., Lai, E.C., 2013. Homeostatic control of Argonaute stability by microRNA availability. Nat. Struct. Mol. Biol. 20, 789–795.

Spratford, C.M., Kumar, J.P., 2015. Extramacrochaetae functions in dorsal-ventral patterning of Drosophila imaginal discs. Development 142, 1006–1015.

Thurmond, J., Goodman, J.L., Strelets, V.B., Attrill, H., Granates, L.S., Marygold, S.J., Matthews, B.B., Millburn, G., Antonazzo, G., Trovisco, V., Kaufman, T.C., Calvi, B.R., the Flybase Consortium, 2019. FlyBase 2.0: the next generation. Nucleic Acids Res. 47, D759–D765.

Troost, T., Schneider, M., Klein, T., 2015. A re-examination of the selection of the sensory organ precursor of the bristle sensilla of Drosophila melanogaster. PLoS Genet. 11, e1004911.

Venken, K.J., Carlson, J.W., Schulze, K.L., Pan, H., He, Y., Spokony, R., Wan, K.H., Koriabine, M., de Jong, P.J., White, K.P., Bellen, H.J., Hoskins, R.A., 2009. Versatile P [acman] BAC libraries for transgenesis studies in *Drosophila melanogaster*. Nat. Methods 6, 431–434.

Wang, L.H., Baker, N.E., 2015. E proteins and ID proteins: helix-loop-helix partners in development and disease. Dev. Cell 35, 269–280.

Zaharieva, E., Haussmann, I.U., Brauer, U., Soller, M., 2015. Concentration and localization of coexpressed ELAV/Hu proteins control specificity of mRNA processing. Mol. Cell Biol. 35, 3104–3115.